

# Structure of the atmospheric convective layer in the tropical zone of the Indian Ocean based on the lidar sensing data

M.S. Permyakov,\* O.A. Bukin,\*\* A.A. Il'in,\*\* V.N. Marichev, and I.G. Nagornyi\*

\* *V.I. Il'ichev Pacific Oceanological Institute,  
Far East Branch of the Russian Academy of Sciences, Vladivostok*

\*\* *G.I. Nevel'skoi Marine State University, Vladivostok  
Institute of Atmospheric Optics,*

*Siberian Branch of the Russian Academy of Sciences, Tomsk*

Received October 4, 2004

The results of lidar sensing of the lower atmosphere in the tropical zone of the Indian Ocean are described. Analysis of lidar data has made it possible to reconstruct and interpret the altitude structure of the atmospheric boundary layer and to follow its nighttime evolution. It is shown that the relative time variability of lidar returns enables one to differentiate in the convective atmospheric boundary layer the condensation level and the inversion layer, to which its maxima in the vertical behavior correspond. The behavior of deviations from the smoothed in time lidar returns has revealed the presence of characteristic zones with reduced negative values in the vicinity of clouds, which can be interpreted as zones of descending motions or the regions of air entraining from the free atmosphere over the inversion. The connection of signal anomalies in the atmospheric boundary layer of 100–300 m and at overlying levels has been followed.

## Introduction

Over the ocean torrid zone, under conditions, unperturbed by synoptic weather systems, the convective atmospheric boundary layer (ABL) is commonly observed, which is clearly defined in the vertical structure of meteorological elements and limited from above by a rather thin stable inversion layer. The ABL structure, its vertical scales, and temporal variability, to a great extent determine the processes of interaction between the ocean and the atmosphere, as well as thermohydrodynamic processes in the middle and upper atmosphere. The ABL characteristics in the tropical latitudes of oceans determine, in a large part, the development of intense weather systems in the tropics, i.e., tropical cyclones and climate throughout the world. Therefore, the ABL over tropical oceans since the 1950s is an object of intense instrumental and theoretical studies, as well as numerical modeling.

Most of data on the ABL structure over oceans were obtained using direct measurements with standard meteorological balloons. Such measurements have a limited vertical and time resolution. In recent decades, lidar methods have found an increasing use in investigations of the structure and dynamics of planetary boundary layers.<sup>1–5</sup> However, as a rule, the lidar measurements are limited by stationary stations located on continents and coasts. Lidar measurements in the open ocean are few in number and accidental. Among the investigations, complex studies in the framework of the project INDOEX<sup>6</sup> should be mentioned, carried out during the period of winter monsoon (January–March, 1999) in the Indian Ocean. These were measurements, among them lidar, of

meteorological, optical, and aerosol characteristics of the atmosphere over the tropical ocean.

In this paper, we present some results of shipborne lidar measurements carried out in the tropics of the northern part of the Indian Ocean in the voyage round the world of a sailing Research Vessel *Nadezhda* in March 2003.

## Description of measurement regions and the equipment

We present the measurements obtained in the Indian Ocean in the 5°–10°N region. The expedition route in the indicated region is given in Fig. 1.

The measurements were conducted in the morning, in the evening and at night, in the vessel motion (the motion velocity at this part of the route did not exceed 4 knots) at the following lidar parameters: laser radiation power in a pulse of 180 mJ, radiation wavelength of 532 nm, pulse length of 5 ns, pulse repetition rate of 10 Hz, and diameter of the receiving objective of 30 cm. Two channels were used for the near (up to 8 km) and far (more than 8 km) zones. In the first channel, a signal from the FEU-79 photomultiplier tube was recorded in the integral regime, then the signal came to the 8-bit analog-to-digital converter; a minimal space resolution was 1.5 m (here we present the measurements with a space resolution of 6 m). In the second channel, a signal from the FEU-136 photomultiplier tube was recorded in the photon counting regime, in which the signal came to a pulse amplifier–shaper and then to a photon counter. The spatial resolution in this channel was 240 m.

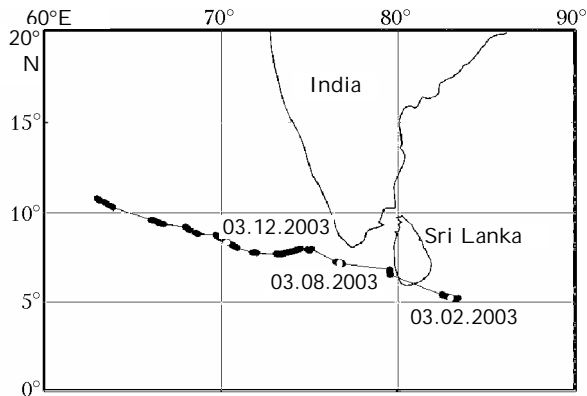


Fig. 1. The route of the vessel *Nadezhda* in the northern region of the Indian Ocean (continuous thin line) and regions of lidar measurements (bold lines).

In the expedition, at regular intervals (6 hours) we conducted measurements of standard meteorological parameters: the air pressure, air and ocean surface temperatures, humidity, and wind. Based on these data, we calculated main parameters of the energy–mass exchange in the ocean–atmosphere system necessary for interpreting lidar measurements in the atmospheric boundary layer.

As a whole, meteorological conditions during the expedition period were determined by a monsoon character of the general atmospheric circulation in the northern area of Indian Ocean and did not differ from the average climatic conditions and conditions in individual years.<sup>7,8</sup> No some significant synoptic atmospheric disturbances were observed in this region of the Indian Ocean. Thus, only weak variations of the atmospheric pressure connected with semidiurnal atmospheric influxes were well defined in continuous records. Typical for this season, weak winds of 1–5 m/s in a north-eastern direction were mainly observed. The sea surface temperature varied over a period of lidar observations from 28 to 31°C, and the relative air humidity varied from 70 to 80% at a mean value of 75% typical for March in the region of measurements. At night, the difference of water and air temperatures varied within 0.1–1.6°C that corresponds to conditions of weak convective instability of the near-water air.

### Methods of the data analysis

The basic problems of lidar data processing from the viewpoint of the convective ABL structure analysis are: to determine the ABL height or the inversion height; to differentiate the entrainment zones (or zones of mixing of air from the convective layer and air from the upper relatively dry and pure atmosphere); to determine the height of the condensation level; to recognize zones with anomalous space–time characteristics of lidar returns; to trace the dynamics of ABL structural elements at nighttime.

Key parameters in theoretical analysis of processes in ABL and in the numerical simulation are the height (of inversion) of the inversion layer and its

thickness (or the thickness of the entrainment layer). Methods of determination of these parameters from the lidar data are considered, for example, in Refs. 5 and 9. However, it should be noted that in these works the inversion (or zone of entrainment) is differentiated at the backscattering vertical profile (individual or mean), whereas these objects are characteristic of a random process, and some statistical procedures are necessary to determine and quantify them. In this paper we realize such an approach when analyzing the vertical behavior of time variability of lidar returns.

Analysis of the ABL structure was made directly by lidar returns without using any conversion procedures of a laser sensing equation for their interpretation. The lidar returns were accumulated in a sliding window (2 minutes) with the window shift to a half of its width and were vertically smoothed out by a filter with a Gaussian kernel of a 18-m half-width. Using all such profiles obtained during the night, we determined the profile of the minimal signal, relative to which the analysis of all profiles was conducted. This procedure allowed us to follow rather fine peculiarities in time behavior of the vertical sensing, such as individual small cumulus clouds up to 100 m in a horizontal direction and to obtain estimates of basic statistical characteristics of signals on the window temporal scales.

We also have analyzed the convective layer structure with the use of procedures of assessment of temporal variability of signals at a particular height. The temporal variability was determined at each height as the ratio between the rms deviation of the signal and its mean at a definite time interval. As a rule, local maxima in the height behavior of temporal variability correspond to layer boundaries with anomalous conditions of backscattering (aerosol, drop). This makes it possible to distinguish the upper and lower cloud boundaries and, as it is shown below, to determine even the height of inversion and the condensation level in the absence of cloudiness. The latter is not identified practically by the vertical behavior of the scattered signal because the integrated characteristics of droplet spectra, and, consequently, the scattering cross section vary very smoothly with height at the condensation level or at the lower cloud boundary.<sup>10</sup> It is also shown<sup>10</sup> with the use of the measured droplet spectra that at the upper and lower cloud boundaries the relative variability of the scattering cross section has extreme values, and we use this fact when interpreting lidar data.

Rather fine peculiarities in the ABL structure are found in the scattered signal deviations from its time-smoothed behavior. Analysis of such deviations allows one to find individual structural elements in the time behavior (or in a horizontal direction with taking account of the motion of the vessel and the wind) and to estimate their typical scales.

Figure 2 schematically shows the ABL convective structure, the process of forming entrainment zones<sup>9</sup> and clarifies the appearance of anomalies in the temporal (or spatial) behavior of the backscattered signal.

Regions of lowered scattering (negative anomalies in the signal deviations) can originate in areas of entrainment of relatively dry air practically without droplet moisture from the free atmosphere above the convective layer or close to individual clouds in zones of descending motions, where partial droplet evaporation occurs and the backscattered signal decreases.

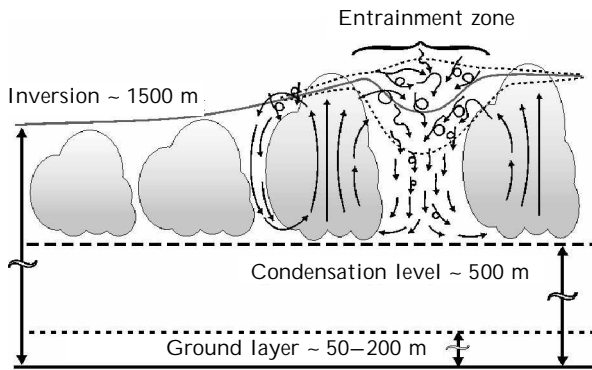


Fig. 2. Structures of the atmospheric boundary layer over the ocean and entrainment zones.

### Results and discussion

Below we give some specific examples of application of the described approach to analysis of the night convective ABL. Of all data on the Indian Ocean, we present situations most typical for the tropics. During all nights of measurements, as a rule, we observed low “friable” individual cumulus clouds and low stratocumulus with small optical thickness at gentle breeze or calm. Strong cumulus clouds of vertical evolution typical for cyclonic weather systems in the tropical zone, were not observed.

First of all, consider an example of behavior of the backscattering signal (relative to the minimal one, Fig. 3a), its deviations from a time-smoothed one (Fig. 3b), and the vertical profile of time variability (Fig. 3c) for a three-hour fragment of lidar observations at a very light night of March 8, when the clouds were not observed visually during measurements. This night, a lidar return was comparatively weak, but in the pattern of temporal behavior we could observe clearly defined layers near the levels of 500 m and 1700 m. The first level corresponds to the condensation level, which height was estimated by the temperature and humidity of the near-water air, varied in the range from 390 m to 480 m. The second layer is identified as the inversion layer. These levels are well-defined by the corresponding maxima in the profile of the signal relative time variability for three hours.

Note the signal variability in the near-water layer up to 200 m–300 m, which we attribute to convective processes in air above the relatively warm water. A local maximum is also observed in this layer in the variability profile.

Figure 4a shows an example of lidar observation of the night behavior of the convective cloudiness in the ABL on the 12th of March. Figure 4b shows the

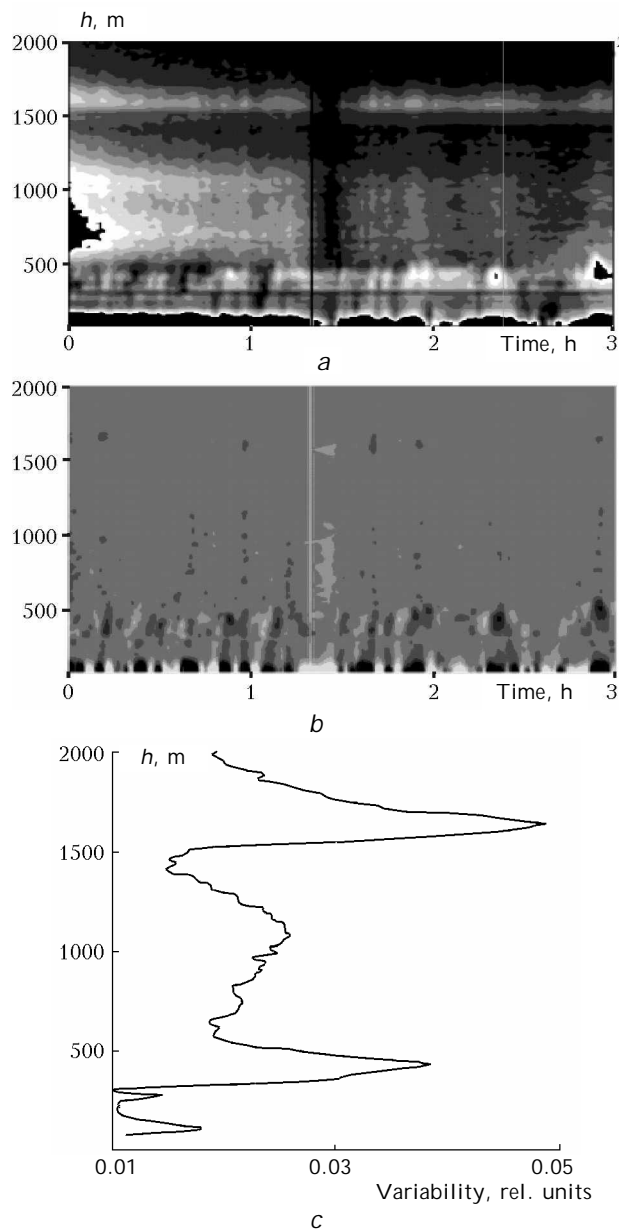


Fig. 3. Night behavior of a lidar return relative to the minimal one (a); deviation of the lidar return from the time-smoothed one (b); the vertical profile of the time variability (c).

night behavior of height peaks in the signal variability. After the sunset, the radiation cooling of air in the ABL results in the progressive increase of the difference of water-air temperatures during night, as well as in the convection amplification in the lower boundary layer and in the entire ABL. By the end of night, the cloudiness occupies the entire layer from the condensation level to the inversion. Individual clouds penetrate the layer above the inversion. Figure 4a shows that at the beginning of night only individual semi-transparent clouds are observed close to the condensation level (by meteorological data of 610–700 m), in the middle of night the cloud tops (where usually the maximal values

of water content and backscattering are observed) reach the inversion layer at a height of 1300 m.

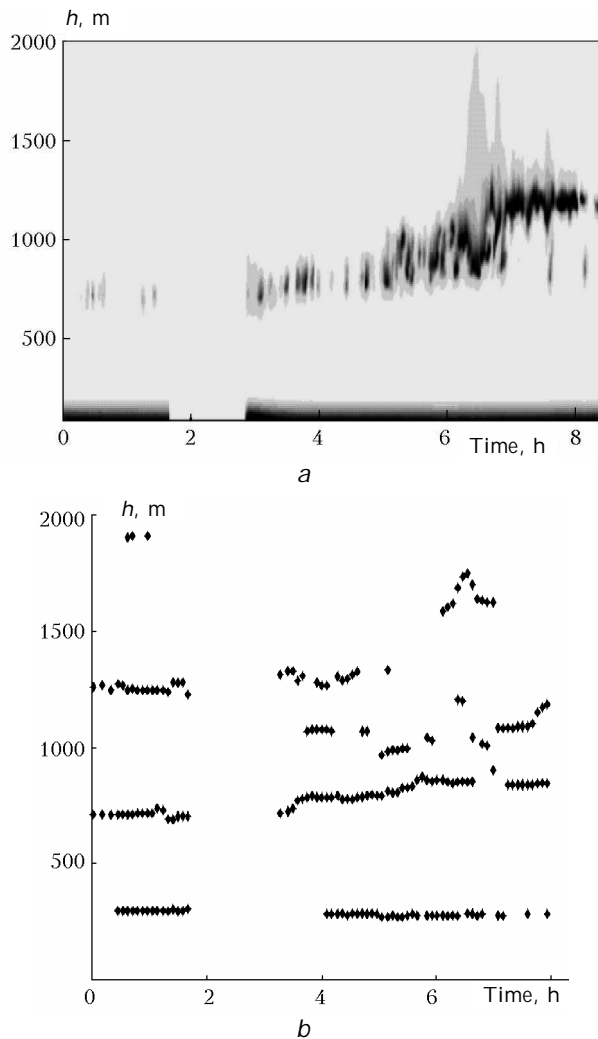


Fig. 4. Night behavior of a lidar return on March 12 (a); the corresponding behavior of altitudes of time variability maxima (b).

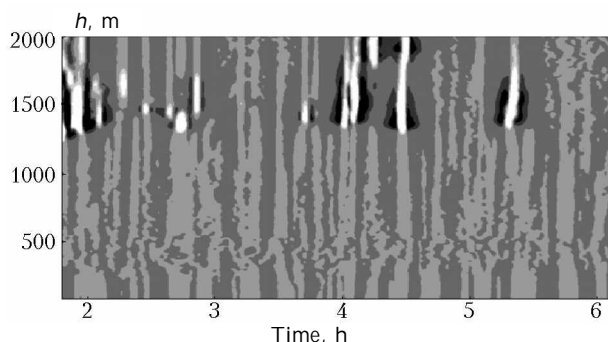


Fig. 5. Fine structure of the convective layer.

Figure 5 shows the fine structure of the convective layer manifesting itself in the signal deviation at each level from the time-smoothed one by the Gaussian filter with a half-width of 12 minutes, at the second half of night on March, 2. Regions of lowering (dark)

of the backscattering signal close to the clouds (almost white shade) are clearly defined, tops of which are concentrated near the inversion layer at altitudes of about 1400–1500 m. The occurrence of black regions, which are symmetric about the kernel of the increased scattering zone (white regions) is caused by processes of entrainment at the inversion altitudes or by descending air flows (see Fig. 2). A connection of cloud structures with the entire ABL structures is seen up to the ground layer.

## Conclusion

Thus, the analysis of lidar data has made it possible to reconstruct and interpret the altitude structure of ABL, as well as to follow its night-time evolution above tropical regions of the Indian Ocean.

It is shown that the relative temporal variability of lidar returns enables one to recognize in the convective layer the condensation level and the inversion layer, to which its maxima in the vertical behavior correspond. The behavior of deviations from the time-smoothed lidar signals has revealed, in the vicinity of clouds, typical zones with the reduced negative values, which can be interpreted as zones of descending air flows or zones of air entrainment from the free atmosphere above the inversion. A relation between signal anomalies in the surface layer of 100–300 m and those at higher levels has been found.

## Acknowledgments

This work was supported by grants of FCP "Integratsiya" E013 "Far-East Floating University," Complex Integration Project "Experimental investigations of effects of space-physical and geophysical disturbances on aerosol formation in the middle and upper atmospheres," and the Russian Foundation for Basic Research (Grant No. 03–05–65219).

## References

1. Yu.S. Balin and A.D. Ershov, *Atmos. Oceanic Opt.* 13, Nos. 6–7, 586–591 (2000).
2. Yu.S. Balin and A.D. Ershov, *Atmos. Oceanic Opt.* 12, No. 7, 592–599 (1999).
3. I.C. Kaimal, U.L. Abshire, R.B. Chadwick, et al., *J. Appl. Meteorol.* 21, 1233–1247 (1982).
4. R. Boers, E.W. Eloranta, and R.L. Coulter, *J. Climate Appl. Meteorol.* 23, 247–266 (1984).
5. S.A. Cohn and W.M. Angevine, *J. Appl. Meteorol.* 39, 1233–1247 (2000).
6. V. Ramanathan, P.J. Crutzen, J. Lelieveld, et al., *J. Geophys. Res.* D 106, No. 22, 28,371–28,398 (2001).
7. G.S. Bhat, M.A. Thomas, J.V.S. Rain, et al., *Boundary-Layer Meteorol.* 106, 263–281 (2003).
8. J.F.L. Verner, D.R. Sikka, and J.M. Robert, G. Stossmeister, and M. Zachariasse, *J. Geophys. Res.* D 106, No. 22, 28,399–28,413 (2001).
9. P. Hageli, D.G. Steyn, and K.B. Strawbridge, *Boundary-Layer Meteorol.* 97, 47–71 (2000).
10. V.R. Noonkester, *J. Atmos. Sci.* 42, No. 11, 1161–1171 (1985).